ELSEVIER

EPR study of polyaniline highly doped by *p*-toluenesulfonic acid

V.I. Krinichnyi [a],[*], H.-K. Roth [b], M. Schrödner [b], B. Wessling [c]

[a] *Institute of Problems of Chemical Physics, Semenov Avenue 1, Chernogolovka 142432, Russia*
[b] *TITK Institute Rudolstadt, Physical Materials Research, Breitscheidstrasse 97, Rudolstadt D-07407, Germany*
[c] *Ormecon GmbH. Ferdinand-Harten-Strasse 7, Ahrensburg D-22926, Germany*

Abstract

Magnetic, relaxation and electronic dynamic parameters of paramagnetic centers in crystalline domains of polyaniline highly doped by *p*-toluenesulfonic acid (PANI-PTSA) as well as PANI-PTSA dispersed in poly(methyl methacrylate) (PANI-PTSA/PMMA) were studied by the 3-cm (9.7 GHz) and 2-mm (140 GHz) wavebands EPR. At both wavebands these polymers demonstrate the Lorentzian single line with the Dysonian contribution indicating intrinsic conductivity of metal-like domains ca. 1500–4000 S/cm at room temperature. Effective conductivity of the polymer is defined by Q3D delocalization of charge carriers within such domains and their Mott variable range hopping between the domains dominating its micro- and macroscopic conductivity. It was shown that the interaction of the charge carriers with the lattice phonons governs the intradomain charge transfer at high temperatures. Dimensionality of the system increases with the polymer dispersion in an insulating matrix. Dipole–dipole interaction of polarons with oxygen biradicals reversibly changes the relaxation of the spins in the initial and dispersed polymers. These paramagnetic centers strongly interact below and weakly above critical temperature T_c of the phase transition that leads to an extremal temperature dependence of the polymer linewidth. The dependence of T_c on electron precession frequency and/or on the PANI-PTSA dispersion in an insulating matrix was revealed. Spin relaxation and dynamics were analyzed to be non-correlated with charge transfer in PANI-PTSA that contradicts the "single conducting chain" model and justifies the formation of Q3D metal-like domains.
© 2006 Elsevier Ltd. All rights reserved.

*Keywords:* Electron paramagnetic resonance; Polyaniline; Polaron

1. Introduction

Doped polyaniline (PANI-ES, the emeraldine salt form, chemical structure in Scheme 1) and its derivatives possess high conductivity and are characterized by unusual spectroscopic and magnetic properties [1,2], attributed to the presence of polarons [3,4]. In contrast to other conducting polymers, the presence of the nitrogen nuclear in the PANI backbone stipulates the phenyl ring rotation near the polymer main *X*-axis and, therefore, leads to unique properties of this polymer [5]. Two main conceptions of charge transfer in doped PANI are now considered. The first one considers elemental charge transfer along and between solitary polymer chains by polaron possessing spin $S = 1/2$ [6,7]. However, Kivelson and Heeger suggested [8] that the interchain interaction in highly doped conducting polymers could suppress the Peierls instability and avoid 1D localization [9] due to significant interchain coherence. According to the alternative theory [10,11], polymer doping leads to the increase in its amorphous phase in number and size of metal-like domains with strongly coupled chains, in which the polarons are localized and charge is transferred by 3D delocalized electrons. The formation of such quasi-three-dimensional (Q3D) crystal domains in the polymer is justified by the increase in its Pauli susceptibility during PANI doping. In the framework of the second approach, electronic and dynamic properties of the polymer are defined mainly by Q3D intradomain and Q1D interdomain charge transfers. As in case of other conducting polymers, the energy levels of polarons localized in the crystal phase of PANI are

* Corresponding author. Tel.: +7 496 522 1714; fax: +7 496 515 5420.
E-mail address: kivi@cat.icp.ac.ru (V.I. Krinichnyi).
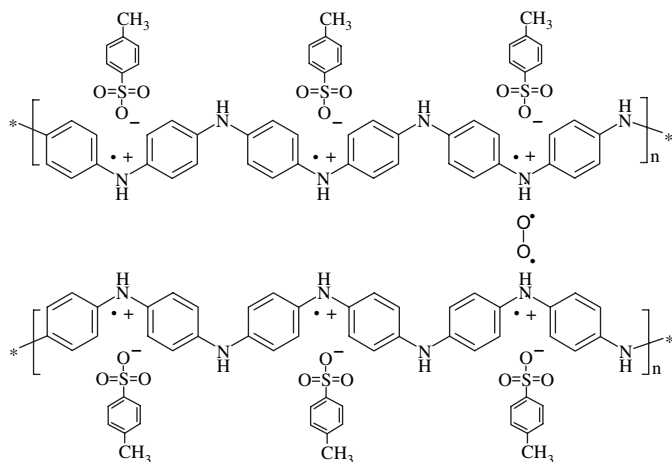
Scheme 1. Schematic structure of emeraldine salt form of polyaniline fully doped by *p*-toluenesulfonic acid. The possible interaction of the >NH groups with •O−O• biradical via hydrogen bond formation is shown.

merged into metal-like band and, therefore, so-called polaron lattice is formed [12,13]. This system is characterized as a ''Fermi glass'', in which the electronic states at the Fermi energy ε_F are localized due to disorder and charge is transferred by the phonon-assisted Mott variable range hopping (VRH) between exponentially localized states near the Fermi level [14]. In some cases diamagnetic bipolarons [15], each possessing two elemental charges, can also be formed in highly doped polymer. Such PANI can be considered as a disordered system on the metal−insulator boundary in which charge is transferred according to the modified Drude model [13]. This model predicts intrinsic conductivity of the Q3D domains to be ca. 10^7 S/cm, however, the experimental value does not exceed 10^3 S/cm [16]. Thus there appears to be a mechanism in the polymers that can diminish even the intrinsic scattering of carriers by thermally excited phonons that limit the conductivity of good metals. The most plausible mechanism for this suppression of scattering by phonons in metallic regions is the Q1D conduction along polymer chains [8,17]. According to this approach, carriers can be scattered only back along the chains that requires phonons of relatively high energy, which are not higher than $k_B T \approx 0.026$ eV (here k_B is the Boltzmann constant) below room temperature. Hence, conductivity should drop rather sharply at temperatures corresponding to $2k_F$, where k_F is the Fermi wavevector. The mechanism and dynamics of charge transfer in heavily doped PANI are sufficiently dependent on the method of the polymer synthesis and on the dopant nature. For instance, the Fermi level in PANI doped by sulfuric acid lies in the region of localized states, therefore, is considered as a Fermi glass with localized electronic states [18], whereas in PANI-camphorsulfonic acid ε_F lies in the region of extended states governing metal behavior of the latter near the metal−insulator boundary [19,20].

PANI doped with *para*-toluenesulfonic acid (PANI-PTSA, Scheme 1) and its dispersion in poly(methyl methacrylate) (PANI-PTSA/PMMA) yield the density of states at the Fermi level ε_F, $n(\varepsilon_F) \sim 10-20$ states per eV per 2 rings [21–23], that is an order of magnitude greater as compared with the value

obtained for PANI-ES with other counterions [24]. As PANI-PTSA is dispersed in PMMA, the Ph−N−Ph dihedral angle in PANI-ES domains with an averaged diameter of 8 nm [25] decreases from 166° down to 134° [26] that leads to the increase in σ_{dc} [25,27]. Intrinsic conductivity and the mechanism of charge transfer in these metal-like domains have not been studied so far.

The polarons in conducting polymers are characterized by electron spin $S = 1/2$. Thus, the comparatively low-frequency ($\omega_e/2\pi = \nu_e \leq 10$ GHz) [28,29] and especially high-frequency ($\nu_e = 140$ GHz) [30–32] EPR methods are widely used for the study of such systems. Higher spectral resolution and sensibility of the latter allowed us to study various magnetic and electronic properties of different conducting polymers [30–32], PANI among them [33,34]. It was estimated that the polarons localized on short PANI chains prevail in its amorphous phase. The number and mobility of these charge carriers increase as the polymer is slightly doped by different acids that leads to the increase of probability of charge transfer along and between polymer chains and, therefore, to the increase in polymer effective *dc* and *ac* conductivities. The formation of metal-like domains results in a strong interaction of charge carriers with lattice optical phonons and also in dipole−dipole interaction between spins. This leads to the localization of main polarons and to exchange narrowing of their EPR line.

The presence of oxygen molecules in PANI can also affect its magnetic and relaxation parameters due to dipole−dipole interaction of the polarons with the oxygen biradicals each possessing total spin $S = 1$. It was found [35–38] that oxygen can reversibly broad the EPR spectrum of PANI without remarkable change in its conductivity. However, Kang et al. [39] showed that the air treatment of hydrochloric acid-doped PANI reversibly and simultaneously broadens its EPR spectrum and decreases its *dc* conductivity. Such changes were explained by the decrease in polaron mobility as a result of their interaction with the air. However, the opposite effect, *i.e.* the simultaneous broadening of the EPR spectrum and the rise in *dc* conductivity of the same air-treated polymer, was reported by Houze and Nechtschein [40].

We present the first detailed results on the investigation of magnetic, relaxation and electronic transport properties of a crystalline phase in PANI-PTSA and PANI-PTSA/PMMA mainly by 3-cm and 2-mm wavebands EPR in a wide temperature range. Strong changes in these properties were shown on polymer exposure to air. The nature of charge carries is analyzed and the mechanism of charge transfer is determined from the comparison of experimental data. Spin relaxation and dynamics were analyzed to be non-correlated with charge transfer processes that contradicts the model of ''single conducting chains'' in PANI-ES [6,7] and justifies the formation of the Q3D metal-like domains in heavily doped PANI-PTSA.

2. Experimental

Powder-like Ormecon® PANI-PTSA$_{0.5}$ with the lattice constants $a = 0.44$ nm, $b = 0.60$ nm, and $c = 1.10$ nm was used [26,41]. This sample was dispersed in PMMA using an

appropriate technique under shear condition in melt phase. The volume fraction of PANI-PTSA was 30% in PANI-PTSA/PMMA as estimated from the X-ray measurements. These powders with a characteristic size R of individual particles of 0.0129 ± 0.0014 mm (PANI-PTSA) and 0.098 ± 0.006 mm (PANI-PTSA/PMMA) were mixed with MgO powder (1:3) and then placed into a quartz capillary with the internal diameter of ca. 0.6 mm. Such polymer dilution by an insulating matrix allowed one to avoid possible interaction between its powder particles and additionally to use Mn^{2+} with $g_{eff} = 2.00102$ and $a = 87.4$ G to determine g-factor as well as for the magnetic field sweep scale calibration at the 2-mm waveband EPR. For the analysis of the effect of air on magnetic resonance properties of PC, both vacuum-processed and nitrogen filled, and air-containing polymers were studied.

EPR experiments were performed using mainly 3-cm ($\nu_e = 9.7$ GHz) waveband PS-100X and 2-mm ($\nu_e = 140$ GHz) waveband EPR-05 [31,42,43] spectrometers, both with 100 kHz field ac modulation for phase-lock detection. The 3-cm and 2-mm wavebands' EPR spectra of nitrogen and air-treated samples were registered in the temperature range of 120–320 K and their 3-cm waveband EPR spectra were also registered at 77 K in liquid nitrogen. The total spin concentration in the samples was determined using a $Cu_2SO_4 \cdot 5H_2O$ single crystal standard. Total paramagnetic susceptibility of the samples was determined using double integration of their EPR absorption spectra. EPR spectra were simulated using the Microcal Origin V.7.5776 and Bruker WinEPR SimFonia V.1.25 programs. The uncertainty in the determination of the peak-to-peak linewidth ΔB_{pp} and the value of g-factor were consequently $\pm 2 \times 10^{-2}$ G and $\pm 2 \times 10^{-4}$ at 3-cm waveband EPR and $\pm 5 \times 10^{-2}$ G and $\pm 3 \times 10^{-5}$ at 2-mm waveband EPR.

dc conductivity of the pellet-like samples was measured at 6–300 K using a four-probe technique.

3. Results and discussion

3.1. Magnetic resonance parameters

The nitrogen treated PANI-PTSA and PANI-PTSA/PMMA samples at 3-cm waveband EPR demonstrate Lorentzian exchange-narrowed lines with asymmetry factor A/B (the ratio of intensities of the spectral positive peak to negative one) of 1.03 and 1.25, respectively (Fig. 1). The exposure of the samples to air was observed to lead to the reversible line broadening and the increase in the asymmetry factor up to 1.27 and 1.42, respectively. The asymmetry of the EPR lines may arise due to either unresolved anisotropy of the g-factor or the presence of the Dyson term [44] in the spectrum as a result of the interaction of microwave field with charge carriers inside the skin layer with the thickness δ. To verify these assumptions, the 2-mm waveband EPR spectra of the samples were recorded. It is seen from Fig. 1 that the polymers in this waveband EPR also display a single asymmetric Lorentzian line, whose asymmetry factor increases from 1.68 up to 1.95 (PANI-PTSA) and from 1.46 up to 1.78 (PANI-PTSA/
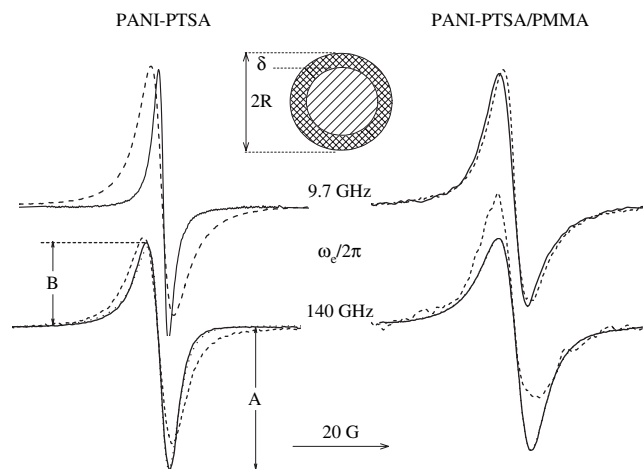

Fig. 1. 3-cm and 2-mm wavebands' EPR spectra of PANI-PTSA and PANI-PTSA/PMMA samples in nitrogen (solid lines) and air (dashed lines) atmosphere. The dotted lines show the spectra calculated from Eq. (1) with $D/A = 0.52$, $\Delta B_{pp} = 4.23$ G (left) and $D/A = 0.29$, $\Delta B_{pp} = 7.98$ G (right). The formation of skin layer of thickness δ on a sample surface with radius R is schematically shown as well.

PMMA) on exposure to air. This fact indicates a substantial interaction of PC even in high fields, the line asymmetry of these PC indeed results from the interaction of microwave field with the charge carriers inside the skin layer. PC with the Dysonian line shape is commonly registered in different highly doped conducting polymers [28–32], PANI among them [33,34]. Such line shape distortion is accompanied by the line shift into higher magnetic fields and the drop in sensitivity of EPR technique. This implies that to determine more correctly and complete such main magnetic resonance parameters as g-factor and peak-to-peak linewidth ΔB_{pp}, one should calculate Dysonian spectra of PC in PANI.

Generally, the Dyson line consists of absorption A and dispersion D terms; therefore, one can write the following equation for its first derivative:

$$\frac{d\chi}{dB} = A\frac{2x}{(1+x^2)^2} + D\frac{1-x^2}{(1+x^2)^2} \qquad (1)$$

where $x = (B - B_0)/\Delta\omega_L$, B_0 is the resonant magnetic field, $\Delta\omega_L = 1/T_2\gamma_e$ is Lorentzian single linewidth, T_2 is the spin–spin relaxation time, and γ_e is the gyromagnetic ratio for electron. The analysis showed that the parameters A and B of the line asymmetry shown in Fig. 1 are correlated with the coefficients A and D of Eq. (1) as $A/B = 1 + 1.45 D/A$.

Some EPR spectra calculated using Eq. (1) are displayed in Fig. 1 by dotted lines. The calculation of the experimental spectra allowed one to determine an effective g-factor for PC in the nitrogen- and air-treated PANI-ES to be equal to 2.00280 and 2.00274, respectively. These values are lower than those obtained for PC localized on six carbon atoms and one nitrogen atom in the repeating unit arising a shift of g-factor of free electron, $g_e = 2.00232$, up to $g \approx 2.0031$ and to $g \approx 2.0054$, respectively [45], so that the spins in the polymers under study are delocalized over some repeating units

each with the size of ca. 0.5 nm. This gives a lower limit of the localization length of electrons in the samples.

3.2. Linewidth

The temperature dependence of the effective absorption peak-to-peak linewidth ΔB_{pp} of the samples determined at both the 3-cm and 2-mm wavebands EPR is given in Fig. 2. It is seen that the ΔB_{pp} value of PC in the PANI samples increases not more than by a factor of two as ν_e increases from 9.7 GHz up to 140 GHz. Such insignificant line broadening with the operating frequency increase was not observed in the studies on other conducting polymers [28—32], including PANI [33,34]. This may be the evidence of a stronger exchange interaction between PC in the polymers under study, which is neither partly nor completely relieved in strong magnetic fields. The linewidth of PC in the PANI-PTSA sample containing nitrogen slightly depends on temperature. At the dispersion of this polymer in PMMA, its linewidth becomes sensitive to temperature (Fig. 2). Air diffusion into the samples leads to the reversible extremal broadening of their EPR line characterized by the critical point T_c (Fig. 2). The increase in the linewidth at the polymer dispersion suggests less motional narrowing [46] and hence, increased localization of PC in PANI-PTSA/PMMA.

The contact of the PANI-ES with the air leads to reversible broadening of its EPR line and also to the extremal temperature dependency of the ΔB_{pp} value with the characteristic temperature T_c (Fig. 2). At the increase of the polarizing frequency from 9.7 GHz up to 140 GHz this value determined for PANI-PTSA and PANI-PTSA/PMMA is shifted from

160 K to 130 K and from 150 K to 120 K, respectively. These effects can probably be described in terms of the Houze—Nechtschein approach [40] postulating the dipole—dipole interaction of the polarons hopping along the solitary polymer chains with the fixed oxygen molecules possessing total spin $S = 1$ (see Scheme 1). The collision of both types of spins should additionally broaden the absorption EPR line by the value

$$\delta(\Delta\omega) = p\omega_{hop}C = \frac{16}{27}\omega_{hop}C\left(1 + \frac{\hbar^2\omega_{hop}^2}{144J^2}\right) \quad (2)$$

where p is the flip-flop probability during a collision of both spins, ω_{hop} is the frequency of the polaron hopping along a polymer chain, C is the number of oxygen molecules per each aniline ring equal to 0.005 for PANI [40], $\hbar = h/2\pi$ is the Planck's constant, and J is the constant of the spin dipole—dipole interaction in the system. If the ratio $J/\hbar$ exceeds the frequency of collision of both types PC, then the condition of strong interaction is realized in the system leading to direct relation of the spin—spin interaction and polaron diffusion frequencies, so that $\lim[\delta(\Delta\omega)] = (16/27)\ C\omega_{hop}$. In an opposite case the condition of weak interaction prevails in the system resulting in an inverse dependence of these frequencies, $\lim[\delta(\Delta\omega)] = 4/3(C/\omega_{hop})(J/\hbar)^2$. According to the spin exchange fundamental concepts [47] the extremal character of the $\delta(\Delta\omega)$ temperature dependency should evidence the realization of both types of spin—spin interaction at $T \leq T_c$ and $T \geq T_c$, respectively. One more reason for the line broadening can be spin localization with the temperature decrease at $T \geq T_c$.
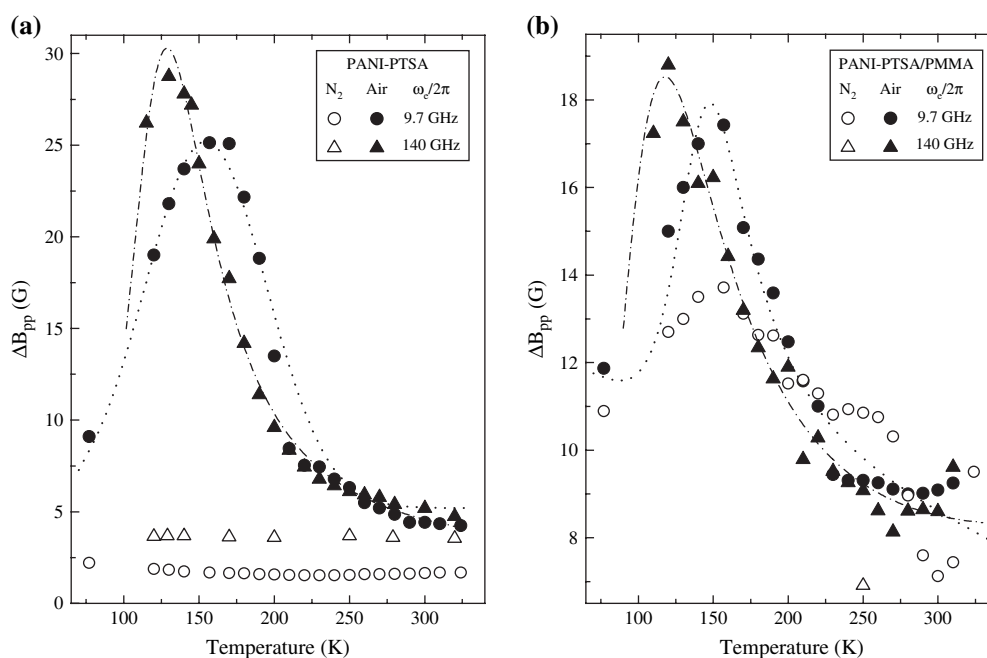

Fig. 2. Temperature dependence of linewidth of PC in PANI-PTSA (a) and PANI-PTSA/PMMA (b) samples filled by nitrogen (open points) and air (filled points) registered at different wavebands EPR. The lines show the dependences calculated from Eq. (2) with $\omega_{lib}^0 = 9.6 \times 10^{17}$ s^{-1}, $E_a = 0.058$ eV, $J = 0.28$ eV (dash-dotted line), $\omega_{lib}^0 = 1.3 \times 10^{19}$ s^{-1}, $E_a = 0.102$ eV, $J = 0.36$ eV (dotted line) (a) and with $\omega_{lib}^0 = 5.8 \times 10^{15}$ s^{-1}, $E_a = 0.031$ eV, $J = 0.015$ eV (dash-dotted line), $\omega_{lib}^0 = 8.1 \times 10^{17}$ s^{-1}, $E_a = 0.090$ eV, $J = 0.041$ eV (dotted line) (b).

As y reach percolation limit, an interaction between polymer chains increases, so that the mobile polarons become localized at the $>$NH site [48]. These groups are available for oxygen of the air and can form hydrogen bond as it is seen in Scheme 1. The concept of hydrogen bonding was also used to explain charge transport in some undoped conducting polymer [49,50] and biological systems [51]. Such a hydrogen bonding can lead to closer packing of its chains and, therefore, to more crystalline structure with localized polarons and Q3D delocalized electronic wave functions [10,11], in analogy with organic ion-radical salts [52]. Therefore, to use this approach we should assume the dipole–dipole interaction of the localized polarons with adsorbed oxygen molecules librating near the polymer chains. Such initial conditions make it possible to apply the chain of argument in the Houze–Nechtschein theory for the interpretation of our data.

Supposing an activation character of small-scale librations of the oxygen molecules near polymer chains with frequency $\omega_{hop} = \omega_{lib} = \omega_{lib}^0 \exp(-E_a/k_B T)$ the $\Delta B_{pp}(T)$ dependencies presented in Fig. 2 were fitted well by Eq. (2) with $E_a = 0.058$ eV, $J = 0.28$ eV and $E_a = 0.102$ eV, $J = 0.36$ eV (Fig. 2a), and with $E_a = 0.031$ eV, $J = 0.015$ eV and $E_a = 0.090$ eV, $J = 0.041$ eV (Fig. 2b). The J values determined sufficiently exceed an appropriate constant of spin collision of nitroxide radicals with paramagnetic ions in liquids, $J \le 0.01$ eV [47]. The dispersion of the initial PANI-PTSA sample in PMMA leads to the decrease in both the J and E_a values. These values additionally decrease with the increase of the registration frequency. Such effects can probably be explained e.g. by the effect of an external magnetic field on the spin exchange process in the polymers under study. The decrease in T_c with the increase of the external magnetic field seems to justify this supposition.

3.3. Spin relaxation and dynamics

As the microwave power increases, the absorption line of the samples shown in Fig. 1 is broadened. Such effect allows one to determine their relaxation parameters using well-known procedure [53]. Effective spin-lattice T_1 and spin–spin T_2 relaxation times determined for the samples under study are presented in Table 1.

If the polarons can really diffuse even in highly doped PANI [7] along and between the polymer chains with respective diffusion coefficients D_{1D} and D_{3D}, they should induce an additional magnetic field in the whereabouts of another spins leading to the acceleration of electron relaxation of the whole spin ensemble. As the relaxation times of the spin reservoir are defined mainly by a dipole–dipole interaction between the spins, the following equations can be written [54]:

$$T_1^{-1}(\omega_e) = \langle \omega^2 \rangle [2J(\omega_e) + 8J(2\omega_e)] \tag{3a}$$

$$T_2^{-1}(\omega_e) = \langle \omega^2 \rangle [3J(0) + 5J(\omega_e) + 2J(2\omega_e)] \tag{3b}$$

where $\langle \omega^2 \rangle = 1/10 \gamma_e^4 \hbar^2 S(S+1) n \sum_{ij}$ is the constant of a dipole–dipole interaction for powder, n is the number of polarons per each monomer unit, $\sum_{ij}$ is the lattice sum for powder-like sample, $J(\omega_e) = (2D_{1D}^| \omega_e)^{-1/2}$ at $D_{1D}^| \gg \omega_e \gg D_{3D}$ or $J(0) = (2D_{1D}^| D_{3D})^{-1/2}$ at $D_{3D} \gg \omega_e$ is a spectral density function for Q1D motion, $D_{1D}^| = 4D_{1D}/L^2$, ω_e is the resonant angular frequency of the electron spin precession, and L is a factor of spin delocalization over a polaron. The similar spectral density function was earlier used in the study of spin dynamics in PANI and other conducting polymers [29–34,55].

The conductivity of a polymer due to the so supposed Q1D and Q3D mobilities of N_p polarons, each transferring e elemental charge, can be determined as

$$\sigma_{1D,3D} = \frac{N_p e^2 D_{1D,3D} d_{1D,3D}^2}{k_B T}, \tag{4}$$

where $d_{1D,3D}$ are corresponding lattice constants.

Both coefficients of hypothetical polaron diffusion in PANI as well as the respective components of the polymer conductivity due to such PC mobility calculated from Eq. (5) at $L \approx 5$ [56] and Eq. (6), respectively, are presented in Table 1 as well. The data show that as PANI-PTSA sample contacts

Table 1
Spin-lattice (T_1) and spin–spin (T_2) relaxation times (in s), spin intrachain (D_{1D}) and interchain (D_{3D}) diffusion rates (in rad/s), conductivity due to possible intrachain (σ_{1D}) and interchain (σ_{3D}) polaron mobility (in S/cm) (the conductivity terms due to joint polaron and bipolaron mobility are presented below the respective values calculated for polarons) as well as the intrinsic conductivity (σ_{ac}, in S/cm) determined from Dysonian EPR spectra for the initial and dispersed PANI samples at $\omega_e/2\pi = 9.7$ GHz and room temperature

Sample	T_1	T_2	D_{1D}	D_{3D}	σ_{1D}	σ_{3D}	σ_{ac}
PANI-PTSA[a]	1.2×10^{-7}	3.1×10^{-8}	9.0×10^7	1.7×10^7	6.3×10^{-5} 1.1×10^{-2}	3.6×10^{-6} 6.4×10^{-4}	1460
PANI-PTSA[b]	1.1×10^{-7}	1.6×10^{-8}	1.9×10^{11}	5.3×10^6	6.7 24.2	5.5×10^{-5} 2.0×10^{-4}	4100
PANI-PTSA/PMMA[a]	1.4×10^{-7}	7.6×10^{-9}	1.9×10^9	7.2×10^5	5.4×10^{-3} 0.24	6.1×10^{-7} 2.7×10^{-5}	120
PANI-PTSA/PMMA[b]	1.1×10^{-6}	7.4×10^{-9}	1.4×10^{12}	1.1×10^4	13.6 178	3.2×10^{-8} 4.2×10^{-7}	210

[a] In nitrogen atmosphere.
[b] In air atmosphere.

with air, the anisotropy of the spin diffusion D_{1D}/D_{3D} and conductivity σ_{1D}/σ_{3D} increases approximately by four orders of magnitude. These ratios additionally increase by an order of magnitude at the dispersion of the initial sample in PMMA. This implies that the exposure of PANI-ES to air and/or its dispersion in PMMA should lead to higher spin delocalization along the polymer chain.

If one supposes the existence of double charged diamagnetic bipolarons additionally to polarons moving with the diffusing coefficients calculated for polarons, the respective effective conductivities can also be evaluated (see Table 1).

3.4. dc conductivity

Fig. 3 shows the change in *dc* conductivity of the PANI-PTSA and PANI-PTSA/PMMA samples as a function of temperature. The analysis of the low-temperature branch of the $\sigma_{dc}(T)$ dependence of both the PANI-PTSA and PANI-PTSA/PMMA samples exposed to air allows one to suppose a realization of the Mott Q1D and Q3D VRH charge transfers through less conducting (disordered, amorphous) regions typical for granular metal [57]. According to this model, the conductivity of the system with dimension d depends on temperature as [58]

$$\sigma_{dc}(T) = \sigma_0 \exp\left[-\left(\frac{T_0^{|,*}}{T}\right)^{1/d+1}\right] \tag{5}$$

where $\sigma_0 = 2\pi e^2 \omega_0 n(\varepsilon_F) b^2 t_0 \tau_i / h^2 s$, $T_0^{|} = 16/[k_B n(\varepsilon_F) z\langle L\rangle]$ at $d=1$ and $T_0^* = 16/[k_B n(\varepsilon_F)\langle L\rangle^3]$ at $d=3$ [59] are the characteristic temperatures, above which conductivity is essentially

defined by the phonon bath, and below which conductivity is defined by the distributional disorder of electron states in space and energy, ω_0 is the upper hopping frequency nearly equal to optical phonon frequency, ω_{ph}, t_0 is the transfer integral equal to 2–3 eV for π-electron, z is a number of the nearest neighbor chains equal to four for PANI [58], $\langle L\rangle$ is the average length of the charge carrier wave function (or localization length), b is the interchain separation, t_0 is the interchain charge transfer integral, τ_i is the mean free time, and s is the average chain cross-sectional area.

The heating of the samples above 270 K leads to decrease in σ_{dc} (Fig. 3). For explanation of this phenomenon the Kivelson–Heeger model [8] of charge carrier scattering on optical lattice phonons proposed for the interpretation of charge transfer in metal-like domains in π-conjugated polymers seems to be more suitable. According to this model, intrinsic conductivity of domains depends on temperature as [8,17]

$$\sigma_{int}(T) = \sigma_0 T \left[\sinh\left(\frac{\hbar\omega_{ph}}{k_B T}\right) - 1\right] \tag{6}$$

where $\sigma_0 = N_e e^2 c^2 M t_0^2 k_B T / 8\pi\hbar^3 \alpha^2$, N_e is the volume density of carriers with elemental charge e, c is the lattice constant, M is the mass of $>$NH group, and α is the electron–phonon interaction constant.

Therefore, effective conductivity σ_{dc} can be described by a superposition of Eqs. (5) and (6) with appropriated coefficients k_1 and k_2

$$\sigma_{dc}^{-1}(T) = k_1 \exp\left[\left(\frac{T_0^{|,*}}{T}\right)^{1/d+1}\right] + k_2 T^{-1}\left[\sinh\left(\frac{\hbar\omega_{ph}}{k_B T}\right) - 1\right]^{-1} \tag{7}$$
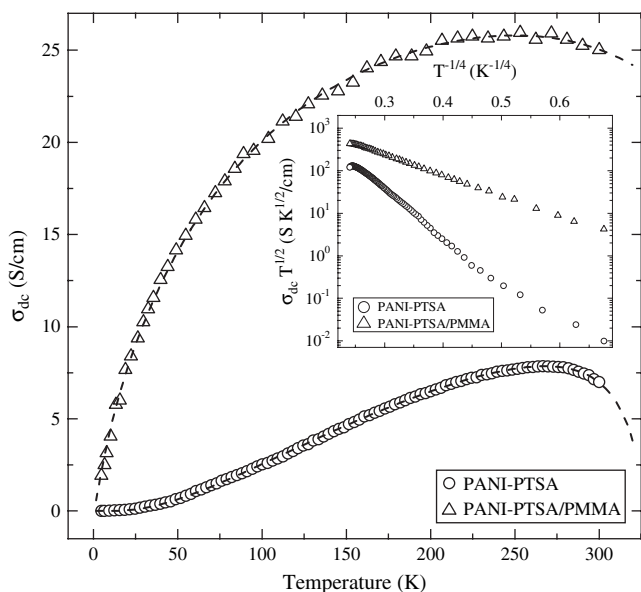

Fig. 3. *dc* conductivity σ_{dc} *vs.* T and $\sigma_{dc}T^{1/2}$ *vs.* $T^{-1/4}$ (inset) of PANI-PTSA and PANI-PTSA/PMMA samples. Top-down lines display the dependences calculated from Eq. (7) with $k_1 = 3.4 \times 10^{-3}$ S/cm, $k_2 = 0.86$ S K/cm, $T_0^* = 1500$ K, $d = 3$, $\hbar\omega_{ph} = 0.032$ eV and $k_1 = 1.3 \times 10^{-2}$ S/cm, $k_2 = 1.8$ S K/cm, $T_0^{|} = 1140$ K, $d = 1$, and $\hbar\omega_{ph} = 0.025$ eV, respectively.

Fig. 3 shows that the experimental data obtained for PANI-PTSA and PANI-PTSA/PMMA samples exposed to air are fitted well by Eq. (7) with $T_0^{|} = 1140$ K, $d = 1$, $\hbar\omega_{ph} = 0.025$ eV and $T_0^* = 1500$ K, $d = 3$, $\hbar\omega_{ph} = 0.032$ eV, respectively. At the dispersion of the PANI-PTSA sample in PMMA its $n(\varepsilon_F)$ value increases from 3 up to 17 states/(eV 2 Ph) [23]. This is accompanied by the appropriate decrease of the charge localization length from 14 nm down to 1.5 nm. The latter value does not exceed the effective radius of the metal-like domain in PANI-PTSA equal to 4 nm [25]. Assuming respective Q1D and Q3D VRH in the nitrogen treated samples, one can determine the analogous decrease in their $\langle L\rangle$ from 59 nm down to 2.3 nm.

The form of Eq. (7) evidences that two successive charge transfers through two regions with lower and higher crystallinities are explicitly realized in the polymers. The most probable distance of the charge carrier hopping in air-containing PANI-PTSA, $R = 1/4(T_0/T)^{1/2}\langle L\rangle$ [58] is 6.8 nm at room temperature. In the framework of the Q1D VRH model the energy of the charge carrier hopping in metal $W = 1/2\,k_B(T_0 T)^{1/2}$ [58] should be near $k_B T$ [57]. W was calculated, for the PANI-PTSA studied, to be 0.025 eV at room temperature lying near $k_B T \approx 0.026$ eV. The velocity of charge carrier, $v_F = 2c/\pi\hbar n(\varepsilon_F)$ [58] near the

Fermi energy level, $\varepsilon_F = 3N_e/2n(\varepsilon_F)$ [60], was determined to be $v_F = 3.7 \times 10^7$ cm s^{-1} and $\varepsilon_F = 0.79$ eV. The latter value lies near the Fermi energy obtained for PANI doped by camphorsulfonic (0.4 eV) [61] and sulfuric (0.5 eV) [33,62–64] acids. Taking the mean free path, l_i, equal to the coherency length in PANI 4.0 nm [12,65], we estimated $\tau_i = 1.3 \times 10^{-13}$ s. The R and W values calculated for Q3D VRH of charge carriers in PANI-PTSA/PMMA are [57,58] $R = [9\langle L\rangle/8\pi k_B T n(\varepsilon_F)]^{1/4} = 1.5$ nm and $W = k_B(T_0 T^3)^{1/4}/2 \approx 0.019$ eV.

The anisotropy of Q1D VRH charge transfer *i.e.* the ratio of mobilities of charge carriers along and between polymer chains, is [58]

$$\frac{\sigma_\parallel}{\sigma_\perp} = \frac{\langle L\rangle}{2k_B T z n(\varepsilon_F)b^2} \tag{8}$$

The anisotropy of *dc* conductivity $\sigma_\parallel/\sigma_\perp$ was determined from the experimental data and was found to decrease from ca. 60 down to 1.2 as the dimension d increased from 1 up to 3 at the PANI-PTSA dispersion in PMMA. The $\langle L\rangle$ values obtained are much greater than the interchain distance in the samples that allows one to point out the 3D character of the metallic states in both the PANI-ES studied. We propose that similar to PANI with other counterions [10,11,33,34,55], PANI-ES in PANI-PTSA can also be considered as a Q1D disordered conductor, which consists of bundles of strongly coupled parallel chains, in which electron wave functions are Q3D delocalized, different from conventional 1D conductors based on organic ion-radical salts [52]. The formation of such bundles is attributed to significant interchain coherence [8] as well as interchain coupling [9,66] that disagrees with the "single conducting chain" models of PANI-ES [6,7].

3.5. ac conductivity

Intrinsic conductivity σ_{ac} and the mechanism of charge transfer in PANI with doping level lying above the percolation threshold depend on the structure and number of counterions introduced into a polymer. At high doping level the saturation of spin-packets decreases significantly due to the increase in direct and cross spin–spin and spin–lattice interactions. Normally, the Dysonian term appears in EPR spectra of such polymers due to the formation of a skin layer on their surface. The shape of the Dysonian EPR line is obviously defined by intrinsic conductivity of the sample, σ_{ac}, that enables one to determine directly this value within a skin layer from its EPR spectrum. In contrast to the saturated dispersion EPR signal, the Dyson-like line shape "feels" dynamics of spin polaron and spinless bipolaron charge carriers diffusing through a skin layer. Since the number and dynamics of each type of charge carriers can differ, electronic dynamic properties of the sample should depend on its doping level.

If the skin layer with thickness δ is formed on the spherical surface with radius R and conductivity σ_{ac}, coefficients A and D in Eq. (1) can be calculated from equations [67]

$$\frac{4A}{9} = \frac{8}{p^4} - \frac{8(\sinh p + \sin p)}{p^3(\cosh p - \cos p)} + \frac{8\sinh p \sin p}{p^2(\cosh p - \cos p)^2}$$
$$+ \frac{(\sinh p - \sin p)}{p(\cosh p - \cos p)} - \frac{(\sinh^2 p - \sin^2 p)}{(\cosh p - \cos p)^2} + 1 \tag{9a}$$

$$\frac{4D}{9} = \frac{8(\sinh p - \sin p)}{p^3(\cosh p - \cos p)} - \frac{4(\sinh^2 p - \sin^2 p)}{p^2(\cosh p - \cos p)^2}$$
$$+ \frac{(\sinh p + \sin p)}{p(\cosh p - \cos p)} - \frac{2\sinh p \sin p}{(\cosh p - \cos p)^2} \tag{9b}$$

where $p = 2R/\delta$ and $\delta = (2/\omega_e\sigma_{ac})^{1/2}$. In the case of $\sigma_{ac} \to 0$ or $\delta \to \infty$ typical for insulator its dispersion term becomes equal to zero, and Eq. (1) is transformed to a simple equation for the first derivative of a symmetrical absorption signal.

Fig. 4 shows the σ_{ac} *vs.* T dependences calculated for the PANI-PTSA and PANI-PTSA/PMMA samples using Eqs. (1) and (9) at different polarizing frequencies. Intrinsic conductivity of the nitrogen treated PANI-PTSA and PANI-PTSA/PMMA samples lies near 1000–1500 S/cm and 40–120 S/cm at room temperature, respectively, and weakly depends on temperature (Fig. 4). As the polymers contact with air, these values increase remarkably (see Table 1) and become more temperature dependent. This can be possibly due to the formation of $>$NH$\cdots$O$-$O$\cdots$HN$<$ bridges with hydrogen bonds (see Scheme 1) that increases the probability of interchain charge transfer. It should be noted that these values sufficiently exceed σ_{1D} and σ_{3D} above calculated that supposes possible Q1D polaron or/and bipolaron diffusion along the "single conducting chain". Further to this approach one should expect $\Delta B_{pp}(T) \propto T_2^{-1}(T) \propto \sigma_{ac}(T)$ [see Eq. (3b)] for the polymers exposed to air. It is seen, however, that the linewidth demonstrates extremal temperature behavior, whereas the σ_{ac} value changes rather monotonically, at least in a high temperature range. Such an extremal shape of the $\Delta B_{pp}(T)$ can, therefore, be explained by the reversible dipole–dipole interaction of localized PC with the oxygen molecules activative librating near the polymer chains assumed above. Such a discrepancy in the $\Delta B_{pp}(T)$ and $\sigma_{ac}(T)$ shapes refutes Q1D charge transfer and justifies the formation of metal-like domains with localized polarons and Q3D delocalized charge carriers in the PANI samples. As in the case of PANI doped with other counterions [33,34], charge dynamics in the samples under study can be interpreted in the frames of the most widely used pair approximation [68] that gives for Q3D charge hopping [57]

$$\sigma_{ac}(T) = \frac{e^2 n^2(\varepsilon_F)\langle L\rangle^3 k_B T\omega_e}{96s}\ln^4\frac{\omega_{ph}}{\omega_e} = \sigma_0 T \tag{10}$$

Fig. 4 shows that *ac* conductivity determined experimentally for PANI-PTSA/PMMA exposed to air and PANI-PTSA containing nitrogen or air from their Dysonian EPR spectra follows well Eq. (10), at least in a high temperature range. Conductivity determined for both samples at 140 GHz was surprisingly lower than that determined at lower
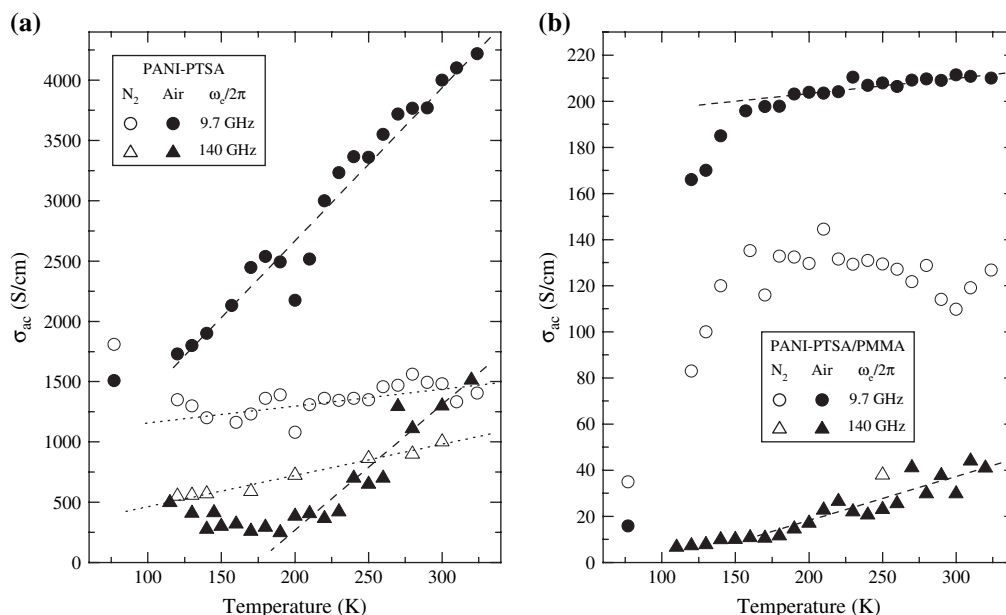
Fig. 4. Temperature dependence of *ac* conductivity of PANI-PTSA (a) and PANI-PTSA/PMMA (b) samples in nitrogen (open symbols) and air (filled symbols) atmosphere determined from their Dysonian spectra registered at different wavebands EPR. Top-down dotted lines in (a) present the dependences calculated from Eq. (10) with $\sigma_0 = 2.0$ S K/cm and $\sigma_0 = 2.6$ S K/cm, respectively. By the top-down dashed lines are shown the dependences calculated from Eq. (10) with, respectively, $\sigma_0 = 12.3$ S K/cm and $\sigma_0 = 9.3$ S K/cm (a) and $\sigma_0 = 0.087$ S K/cm and $\sigma_0 = 0.17$ S K/cm (b).

frequency. This is possibly due to a deeper penetration of microwave radiation quantum with higher energy into the polymer bulk. In this case the σ_{ac} obtained should be rated as a lower limit of intrinsic conductivity at this waveband EPR.

Intrinsic conductivity was calculated for the PANI-PTSA and PANI-PTSA/PMMA samples from Eq. (10) with $\omega_e/2\pi = 9.7$ GHz and $s = 0.05$ nm^2 to be 4.3×10^3 S/cm and 290 S/cm, respectively. These values lie close to those calculated from the Dysonian EPR spectra of these samples (see Table 1). However, these values calculated from Eq. (10) for the air-containing samples with $n(\varepsilon_F)$ equal to 3 and 17 states/(eV 2 Ph) [23] should be equal to 6.8×10^4 S/cm and 3.1×10^3 S/cm, respectively, that is, more than an order of magnitude higher than those presented in Table 1.

4. Conclusions

Multifrequency EPR broadens the self-descriptiveness of the method and allows one to determine fine details of relaxation, conformation and electronic dynamics processes in the initial and dispersed PANI-PTSA low-dimensional organic conductor. PANI-ES contains Q3D high crystalline metal-like domains with significant interchain coherence leading to localized character of polaronic charge carriers. In contrast to other conducting polymers, the interaction between polarons in PANI-ES does not reduce at magnetic field up to 5 T. The formation of metallic domains in PANI-ES is attributed to the significant interchain interaction in the ordered crystalline regions, which avoids Q1D localization. Disordering effects existing in the polymer transform the metallic state characteristic of ideal polymer chains with completely delocalized electrons into the 'Fermi glass' with finite density of

states at the Fermi level. Conductivity of the pure PANI-PTSA sample was defined to be governed by Q3D intradomain and Q1D interdomain charge transfers and the latter is characterized by charge transfer through the regions with different crystallinities. Charge transfer in PANI-PTSA dispersed in an insulating polymer matrix is defined by Q3D inter- and intradomain hopping. The dispersion of initial PANI-PTSA leads to the formation of quasi-metallic domains with a broad 3D energy band and 3D interrelated delocalized electrons surrounded by disordered matrix. This results in less effective *ac* conductivity as compared to pure PANI-PTSA and possibly decreases the height of amorphous barriers. In this system a charge Q3D tunnels from particle to particle through an insulating barrier. PMMA layer hampers the penetration of air to metal-like domains additionally decreasing their intrinsic conductivity. Such a picture agrees with the mesoscopic nanometal concept pointed out polyaniline as granular metal in which the dispersion induced insulator-to-metal transition, however, contradicts the "single conducting chain" models of PANI-ES.

The presence of air is assumed to reduce electrostatic Coulomb interaction between positive charges on the chains and the anions, and, thus, increases delocalization of spins (not polarons as quasi-particles) over the polymer backbone. In PANI-ES filled with air the bridges with hydrogen bonds are formed that result in the increase in its intrinsic conductivity. The dipole–dipole interaction of polarons with the oxygen molecules leads to reversible changes in spin relaxation and depends on the intensity of an external magnetic field. The interaction between these PC decreases with the polymer dispersion in an insulating matrix, and is accompanied with the decrease in the activation energy of spin–spin collisions and in the energy transfer from a spin reservoir to a polymer lattice.

Acknowledgements

References

[1] Syed AA, Dinesan MK. Talanta 1991;38(8):815.

[2] Trivedi DC. In: Nalwa HS, editor. Handbook of organic conductive molecules and polymers, vol. 2. Chichester: John Wiley; 1997. p. 505–72 [chapter 12].

[3] Ginder JM, Epstein AJ, MacDiarmid AG. Synth Met 1989;29(1):E395.

[4] Ginder JM, Epstein AJ. Phys Rev B 1990;41(15):10674.

[5] McCall RP, Ginder JM, Roe MG, Asturias GE, Scherr EM, MacDiarmid AG, et al. Phys Rev B 1989;39(14):10174.

[6] Galvao DS, don Santos DA, Laks B, de Melo CP, Caldas MJ. Phys Rev Lett 1989;63:786.

[7] Mizoguchi K, Nechtschein M, Travers J-P, Menardo C. Phys Rev Lett 1989;63(1):66.

[8] Kivelson S, Heeger AJ. Synth Met 1988;22(4):371.

[9] Firsov YA. In: Fritzsche H, Adler D, editors. Localization and metal insulator transition. New York: Plenum; 1985. p. 471.

[10] Zuo F, Angelopoulos M, MacDiarmid AG, Epstein AJ. Phys Rev B 1987; 36(6):3475.

[11] MacDiarmid AG, Epstein AJ. Faraday Disc 1989;88:317.

[12] Pouget JP, Jozefowicz ME, Epstein AJ, Tang X, MacDiarmid AG. Macromolecules 1991;24(3):779.

[13] Lee K, Heeger AJ. Synth Met 1997;84(1–3):715.

[14] Epstein AJ, Joo J, Kohlman RS, Du G, MacDiarmid AG, Oh EJ, et al. Synth Met 1994;65(2–3):149.

[15] Stafstrom S, Bredas JL, Epstein AJ, Woo HS, Tanner DB, Huang WS, et al. Phys Rev Lett 1987;59(13):1464.

[16] Joo J, Oh EJ, Min G, MacDiarmid AG, Epstein AJ. Synth Met 1995; 69(1–3):251.

[17] Pietronero L. Synth Met 1983;8:225.

[18] Lee K, Heeger AJ, Cao Y. Synth Met 1995;72(1):25.

[19] Reghu M, Cao Y, Moses D, Heeger AJ. Phys Rev B 1993;47(4):1758.

[20] Yoon CO, Reghu M, Moses D, Heeger AJ, Cao Y. Phys Rev B 1993; 48(19):14080.

[21] Srinivasan D, Raghunathan A, Natarajan TS, Rangarajan G, Subramaniam CK, Wessling B. Czech J Phys 1996;46:2035.

[22] Wessling B. In: Nalwa HS, editor. Handbook of organic conductive molecules and polymers, vol. 3. Chichester: John Wiley & Sons; 1997. p. 497–632 [chapter 11].

[23] Raghunathan A, Kahol PK, Ho JC, Chen YY, Yao YD, Lin YS, et al. Phys Rev B 1998;58(24):R15955.

[24] Roth S, Carroll D, editors. One-dimensional metals: conducting polymers, organic crystals, carbon nanotubes. Weinheim: Wiley-VCH; 2004.

[25] Pestler R, Nimtz G, Wessling B. Phys Rev B 1994;49(18):12718.

[26] Wessling B, Srinivasan D, Rangarajan G, Mietzner T, Lennartz W. Eur Phys J E 2000;2(3):207.

[27] Kaiser AB, Subramaniam CK, Gilberd PW, Wessling B. Synth Met 1995; 69(1–3):197.

[28] Bernier P. In: Scotheim TE, editor. Handbook of conducting polymers, vol. 2. New York: Marcel Dekker, Inc; 1986. p. 1099–125 [chapter 30].

[29] Mizoguchi K, Kuroda S. In: Nalwa HS, editor. Handbook of organic conductive molecules and polymers, vol. 3. Chichester, New York: John Wiley & Sons; 1997. p. 251–317 [chapter 6].

[30] Krinichnyi VI. 2-mm wave band EPR spectroscopy of condensed systems. Boca Raton: CRC Press; 1995.

[31] Krinichnyi VI. Synth Met 2000;108(3):173.

[32] Krinichnyi VI. In: Schlick S, editor. Advanced ESR methods in polymer research. New York: Wiley; 2006. p. 540–75 [chapter 12].

[33] Krinichnyi VI, Roth H-K, Hinrichsen G, Lux F, Lüders K. Phys Rev B 2002;65(15):155205.

[34] Krinichnyi VI, Chemerisov SD, Lebedev YS. Phys Rev B 1997; 55(24):16233.

[35] Inoue M, Inoue MB, Castillo-Ortega MM, Mizuno M, Asaji T, Nakamura D. Synth Met 1989;33:355.

[36] Bartle A, Dunsch L, Naarmann H, Schmeisser D, Gopel W. Synth Met 1993;61:167.

[37] Nechtschein M, Genoud F. Solid State Commun 1994;91(6):471.

[38] Kahol PK, Dyakonov AJ, McCormick BJ. Synth Met 1997;84:691.

[39] Kang YS, Lee HJ, Namgoong J, Jung B, Lee H. Polymer 1999;40(9): 2209.

[40] Houze E, Nechtschein M. Phys Rev B 1996;53(21):14309.

[41] Hennessy MJ, McElwee CD, Richards PM. Phys Rev B 1973;7:930.

[42] Galkin AA, Grinberg OY, Dubinskii AA, Kabdin NN, Krymov VN, Kurochkin VI, et al. Instrum Exp Technol 1977;20(4):1229.

[43] Krinichnyi VI. J Biochem Biophys Methods 1991;23(1):1.

[44] Dyson FJ. Phys Rev B 1955;98:349.

[45] Morton JR. Chem Rev 1964;64:453.

[46] Kubo R, Tomita K. J Phys Soc Jpn 1954;9:888.

[47] Molin YN, Salikhov KM, Zamaraev KI. Spin exchange. Berlin: Springer; 1980.

[48] Kahol PK, Dyakonov AJ, McCormick BJ. Synth Met 1997;89(1):17.

[49] Brenneman KR, Epstein AJ, Feng J, Zhou Y, MacDiarmid AG, Kahol PK. Synth Met 1999;101(1–3):785.

[50] Krinichnyi VI, Roth H-K. Appl Magn Reson 2004;26:395.

[51] Davydov AS. Solitons in molecular systems (Russ.). Kiev: Naukova Dumka; 1994.

[52] Williams JM, Ferraro JR, Thorn RJ, Carlson KD, Geiser U, Wang HH, et al. Organic superconductors (including fullerenes): synthesis, structure, properties, and theory. New Jersey, Englewood Cliffs: Prentice-Hall, Inc; 1992.

[53] Poole ChP. Electron spin resonance, a comprehensive treatise on experimental techniques. New York: John Wiley & Sons; 1983.

[54] Carrington F, McLachlan AD. Introduction to magnetic resonance with application to chemistry and chemical physics. New York, Evanston, London: Harrer & Row, Publishers; 1967.

[55] Kon'kin AL, Shtyrlin VG, Garipov RR, Aganov AV, Zakharov AV, Krinichnyi VI, et al. Phys Rev B 2002;66(7):075203.

[56] Devreux F, Genoud F, Nechtschein M, Villeret B. In: Kuzmany H, Mehring M, Roth S, editors. Electronic properties of conjugated polymers, vol. 76. Berlin: Springer-Verlag; 1987. p. 270–6.

[57] Mott NF, Davis EA. Electronic processes in non-crystalline materials. Oxford: Clarendon Press; 1979.

[58] Wang ZH, Ray A, MacDiarmid AG, Epstein AJ. Phys Rev B 1991;43(5): 4373.

[59] Nakhmedov EP, Prigodin VN, Samukhin AN. Sov Phys Solid State 1989; 31:368.

[60] Blakemore JS. Solid state physics. Cambridge: Cambridge University Press; 1985.

[61] Lee KH, Heeger AJ, Cao Y. Phys Rev B 1993;48(20):14884.

[62] Roth H-K, Krinichnyi VI. Makromol Chem Macromol Symp 1993; 72:143.

[63] Krinichnyi VI, Nazarova IB, Goldenberg LM, Roth H-K. Polym Sci A 1998;40(8):835.

[64] Krinichnyi VI. Russ Chem Bull 2000;49(2):207.

[65] Jozefowicz ME, Laversanne R, Javadi HHS, Epstein AJ, Pouget JP, Tang X, et al. Phys Rev B 1989;39(17):12958.

[66] Prigodin VN, Firsov YA, Weller W. Solid State Commun 1986;59: 729.

[67] Chapman AC, Rhodes P, Seymour EFW. Proc Phys Soc 1957; B70(4):345.

[68] Long AR. Adv Phys 1982;31:553.